RGO Technical Note 118
The Measurement of Spatial Resolution in EEV4280 CCD Images

Simon Tulloch. 7 July 1998

CONTENTS

1. Introduction

It is convenient to think of a thinned backside illuminated CCD as being an array of sharply defined individual pixel sensors, the extent of each pixel being defined by the pattern of electrodes at the rear surface of the device. This is not actually the case due to the finite thickness of a CCD and the presence of field free regions in the silicon. Photoelectrons generated close to the surface of the silicon are easily able to diffuse some distance laterally before being collected in adjacent pixels (this effect is referred to as 'Charge Spreading' in this report). The true extent of an individual pixel therefore exceeds its physical size as defined by the lithographic mask used in production, often by a considerable amount. Effective pixel size is also a function of wavelength. Blue photoelectrons are all absorbed in the top few nanometers of silicon and have further to travel before reaching the potential well generated by the backside electrodes. Red photoelectrons are generated more uniformly throughout the depth of the device and on average are collected by this potential well more readily.

Charge Spreading can seriously degrade image resolution. Its effect can be gauged by projecting a sub-pixel diameter pinhole onto the CCD and measuring the Full Width at Half Maximum (FWHM) of the resultant image. If the projected size of the pinhole becomes insignificant with respect to the pixel size then the optical stimulus received by the CCD approaches a delta function. If this delta function is then stepped across the pixel, and the pixel signal read out at each position, the Charge Spreading characteristics can be arrived at. The EEV42-80 CCDS have a pixel size of 13.5µm, and producing an optical stimulus a small fraction of this size is quite challenging. It is made harder by the presence of a 4mm thick cryostat window between light source and CCD.

This report outlines the design of an optical system able to produce sub-pixel diameter optical stimuli and presents some results obtained using it with an EEV42-80 CCD.

2. A New Instrument for Measurement of Spatial Resolution.

The RGO instrument science group already has a spot projector system that is used for coplanarity measurement of CCD cameras (see Technical note 110). The optical quality of the projector head is insufficient to produce sub-pixel spots, necessitating a new design, however, the rest of this system : an X:Y scan stage and a mounting structure for camera cryostats are suitable as elements of a spatial resolution measurement instrument. The old coplanarity scanner, with new optical head installed is shown below :

Fig 1) Spatial Resolution measurement equipment.

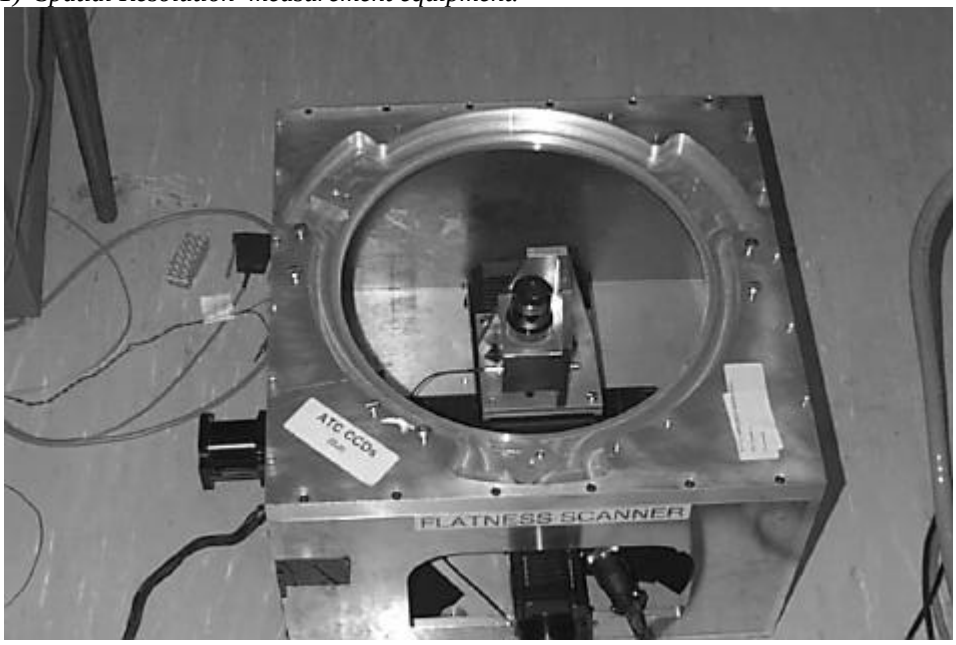

2.1. Optical Design.

A few refractive designs were investigated using the ZEEMAX modelling package but no suitable ones found. The requirement that the instrument work across the wavelength range of a CCD (350nm to 1µm) suggested instead , the use of reflective optical elements. The simplest solution was to use an off the shelf 'Schwarzschild' design microscope objective from Ealing Optics in combination with an LED illuminated pinhole. ZEEMAX showed that even with a 4mm thick cryostat window in the beam, the resultant spot image at the CCD surface would be diffraction limited. The diagram below shows a schematic of the optical head. The light sources are LEDs. These illuminate a diffuse screen which in turn , evenly illuminates a 20µm pin-hole

Fig 2) Spatial resolution measurement optics.

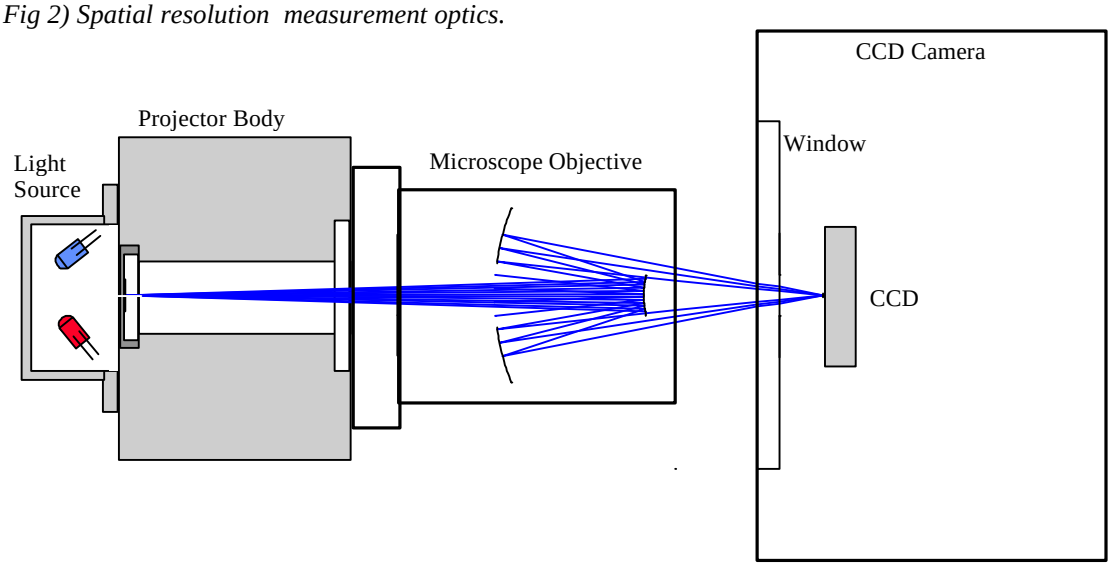

2.2. Mechanical Design.

The new optical head needed a compact design so as to fit into the same space as the coplanarity scanner. Both are shown in the photograph below. They both measure approximately 12 x 12 x 12 cms.

Fig 3) Optical heads for the coplanarity scanner(left) and spatial resolution measurement (right)

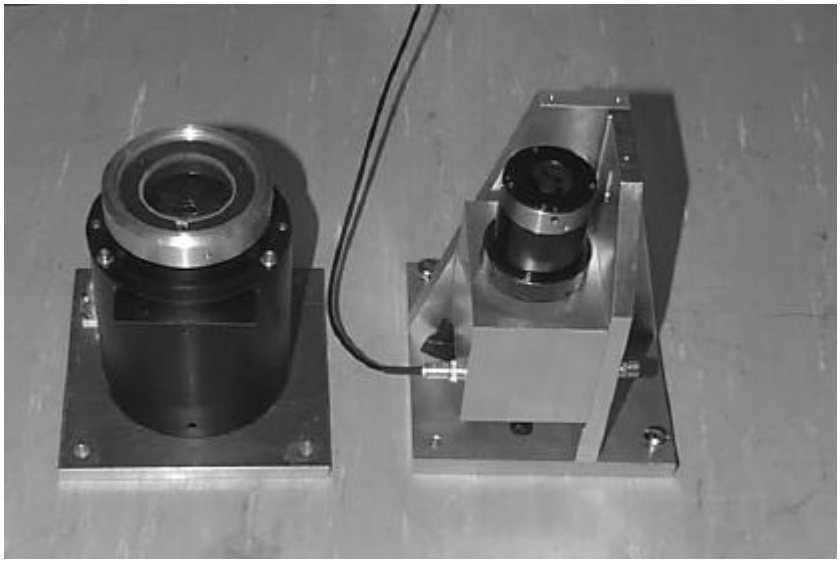

2.3. Optical Performance.

The reflecting microscope objective used in the instrument (Ealing 25-0506) had a Numerical Aperture of 0.28. It projected an approximately f2 beam onto the CCD. This fast system had very critical focusing which was coarsely achieved using adjustments to the faceplate capstans of the CCD camera. The magnification of the system was 0.13, requiring a maximum pinhole diameter of 20μm. Any larger than this and the projected spot diameter would be too large. The Point Spread Function of the system is shown below :

Fig 4) PSF of optics compared to size of a CCD pixel

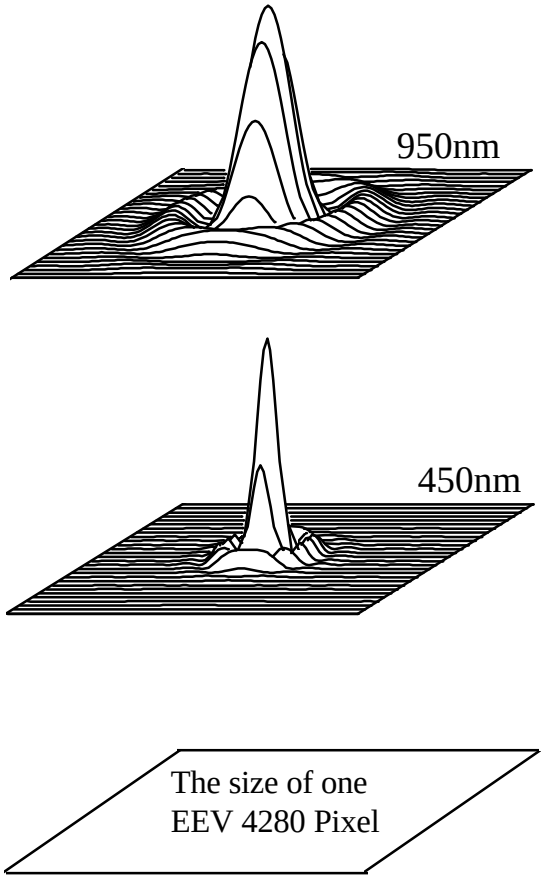

The size of the PSF is tabulated below. The true size of the projected spot will be the PSF convolved with the de-magnified pinhole image. The performance is really only suitable for measurements on EEV CCDs at the shorter wavelengths.

Wavelength (nm)	**Diameter of Airy Disk (μm)**	**Diameter encircling 85% of energy (μm)**	**Diameter encircling 90% of energy (μm)**
380	1.5	3.3	4.9
450	2	3.9	5.8
650	2.8	5.7	8.4
950	4	8.2	12.2

2.4. Practical Operation.

Before any measurements can be made the optics must be very precisely focused. The beam projected from the objective is f2, so even a focus error of 10μm will render it unusable. Generally measurements can be made anywhere on a CCD, the assumption being that the the Charge Spreading characteristics of one pixel is much the same as that of any other. A course focus is first achieved by adjustment to the capstans on the cryostat faceplate, the degree of mis-focus being gauged from inspection of the spot image. When adjusting the capstans they should be rotated in unison so that the faceplate remains roughly horizontal (parallel to the plane of the X-Y stages). At this stage the spot projector should be positioned close to the chip centre. After a few iterations it should be possible to bring the projected spot size down to a diameter of a few tens of pixels, which corresponds to a focus error of a few hundred microns. The cryostat should then be tilted over slightly by moving one capstan clockwise by one turn and another anti-clockwise by one turn. If the line joining these two capstans is parallel to the long axis of the CCD then the centre of the CCD will remain close to focus, the bottom end will be away from focus and the top end also away from focus but in the opposite sense. There should therefore be an intermediate position on the CCD in which the focus error is zero. This point is found by scanning the spot down the long axis of the CCD during image integration. The resultant line image can be examined using IRAF and the FWHM of the line plotted as a function of image row number. The graph below shows a typical result.

Fig 5) Finding best focus

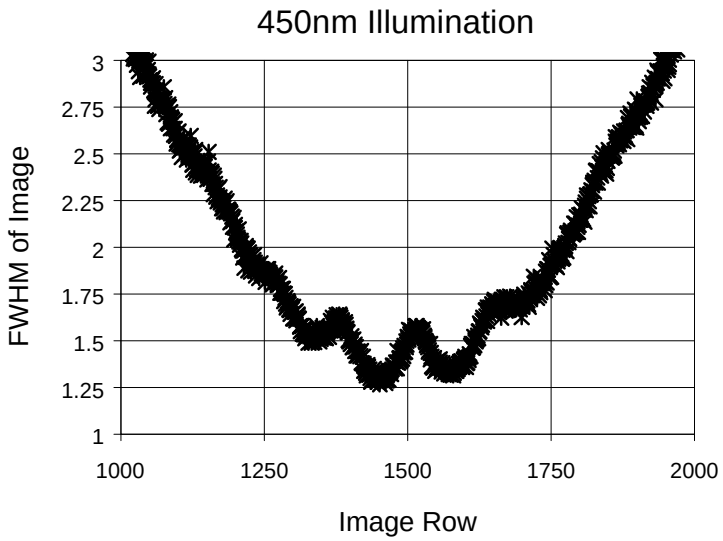

As can be seen the FWHM of the line reaches a minimum close to image row 1500, it is here that perfect focus is found. Further measurements of the CCD characteristics now concentrate on pixels on this part of the chip only. The modulation on the FWHM curve is due to the scan line not being exactly parallel to the CCD columns. More on this in section 3.2.

3. Optical Characteristics of the EEV4280 CCD.

The CCD response was measured at 450 and 650nm, these wavelengths being defined by the peak emissions of the LEDs used to illuminate the pinhole in the spot projector. A 950nm LED was also available but the projected spot size at this wavelength was felt to be too large a fraction of the pixel size to give meaningful results. Three characteristics were measured : Charge Spreading from the pixel response at varying intra-pixel spot positions , the effect of intra-pixel position on the measured width of a spectral line image and the variation in QE with the spot at varying intra-pixel positions.

3.1. Loss of Spatial Resolution due to Charge Spreading.

The image spot was targeted on a pixel centre by moving the translation stages until the wings of the spot image were symmetrical about the central pixel in both the x and y axes (i.e. symmetrical along a row and down a column). The spot was then stepped across the central pixel (see fig 6) and an image recorded at each position. The range of spot positions was varied between +/- 20 microns so as to record data right out in the wings of the pixel response. Two sets of measurements were taken; stepping the spot down an image column and then along an image row. The two sets of data thus recorded could then be analysed to Charge Spreading characteristics in both the X and Y image axes.

Fig 6) Scan Geometry

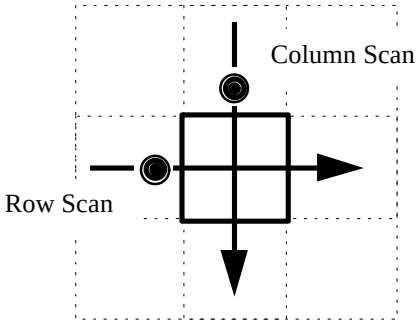

In both types of scan, the spot passed through the pixel centre

The resultant image sets were analysed by first subtracting the image bias and then comparing the signal in the central pixel with the signal in a 7 x 7 pixel array surrounding it. Graphs were then plotted of the central pixel signal as a fraction of total signal, against the spot position. The images also contained further information on intra-pixel quantum efficiency variations; see section 3.3.

Fig 7) Charge Spreading in the EEV4280 at 650nm, in both X and Y image axes.

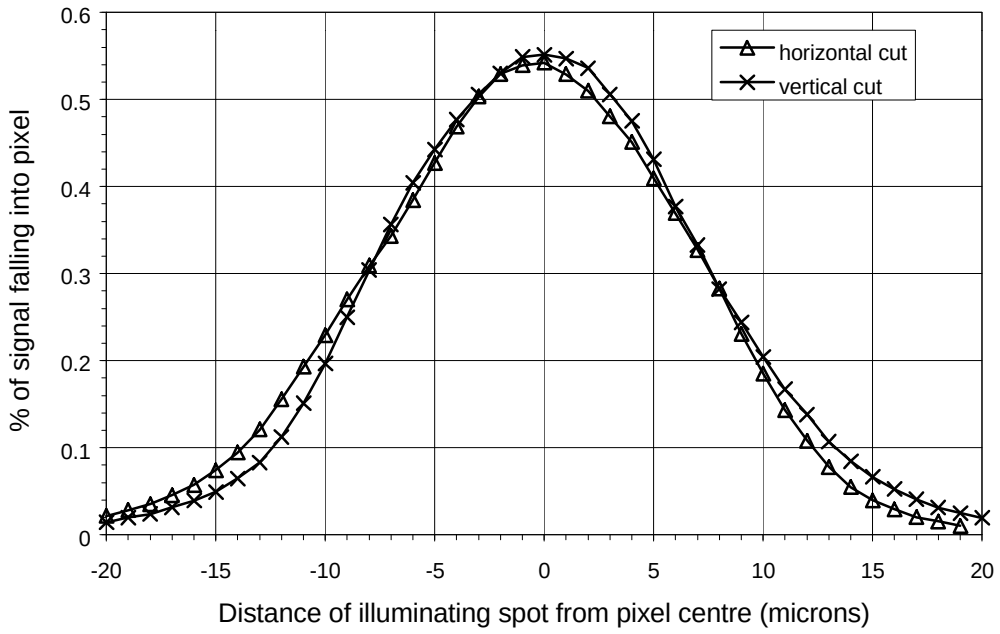

3.2. Line Broadening Variations in Under-sampled Spectra.

In section 2.4, a focusing method was described which involved scanning a line image onto the chip and finding the position where the line width reached a minimum. This line image is essentially the same as a spectral line that would be obtained at a spectrometer port where the projected slit width was of sub-pixel dimension. Figure 5) showed that the measured line-width (using the IRAF 'splot' routine) was actually modulated depending on the intra-pixel position of the line. When the line image fell on a pixel boundary the image size was widened. The width reached a minimum when the image fell at the centre of a pixel. A close up of such a line image is shown below in figure 7).

Fig 7) Close up of a scan line image

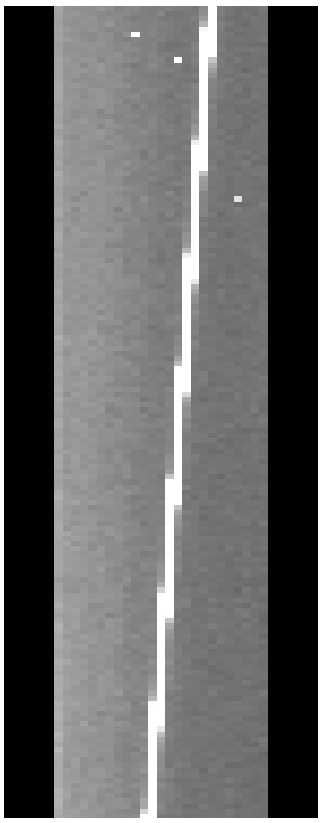

The line width was measured at two wavelengths and is shown in the table below.

Wavelength	**Linewidth width with line image at pixel centre**	**Line Width with line image at pixel boundary**
450nm	1.25 pixels	1.6 pixels
650nm	1.05 pixels	1.3 pixels

Clearly, care must be taken in interpreting the line widths of undersampled spectra.

3.3. Intra-pixel Sensitivity Variations.

The set of images obtained when measuring charge spreading characteristics (section 3.1) could be further analysed to yield QE variations as a function of intra-pixel position. The total signal in each spot image, summed over the entire 7 x 7 pixel image window, was plotted against spot position. This data is presented below in figure 8.

The scatter of points on this graph can be explained by photon noise. The total signal level of the projected spot was 150,000 electrons so in the absence of any Intra-pixel structure the Standard Deviation of the signal would be of the order 0.25%. Any intra-pixel sensitivity variations must be below this level, at least at 650nm.

The vertical grid lines correspond to pixel boundaries. Both a horizontal and a vertical cut through the centres of three adjacent pixels are shown.

Figure 8) Total spot image signal as a function of its position (illumination at 650nm)

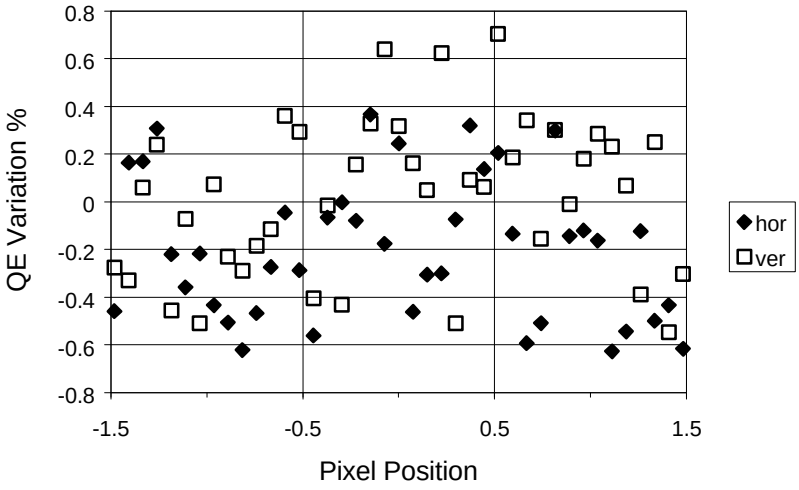

4. Related Papers.

PROC SPIE Instrumentation in Astronomy, Kona, March 1994, **2198**, 836 Jorden, Deltorn, Oates

RGO Technical Note 110, The Design and Use of the RGO CCD Flatness Scanner, June 1997, Tulloch

Appendices.

A. Optical Prescription of the Scanner.

The thickness of Surface 4 is optimised for 950nm illumination. A focus shift of approximately 50μm will occur if 350nm illumination is used.

SURFACE DATA SUMMARY:

Surf	Type	Comment	Radius	Thickness	Glass	Diameter	Conic
OBJ	STANDARD		Infinity	50		0	0
1	STANDARD		Infinity	45.3		7.44	0
STO	STANDARD		16.5928	-27.4	MIRROR	7.3	0
3	STANDARD		43.97439	33.2	MIRROR	32	0
4	STANDARD		Infinity	15.07974		64	0
5	STANDARD		Infinity	4	SILICA	64	0
6	STANDARD		Infinity	8		64	0
IMA	STANDARD		Infinity	0		20	0

B. Possible Method for Higher Resolution Measurements.

By substituting the Ealing objective 25-0555 it will be possible to perform measurements at longer wavelengths. This objective has a higher numerical aperture and can produce smaller spots in the near infra-red. At shorter wavelengths there is little improvement over the existing scanner due to small aberrations in the cryostat window. The distance from the pinhole to the inlet port needs to be about 100mm (in the previous design it was only 50mm) so it is not easily incorporated into the scan box envelope.

Fig 9) Ray Diagram of 25-0555 objective

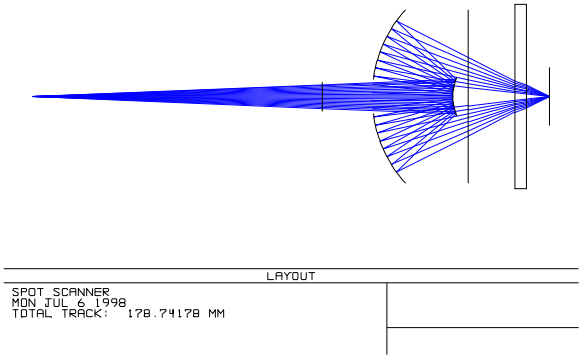

The performance of this objective is summarised below. In the blue the image is no longer diffraction limited and it is not possible to tabulate the Airy Disk diameter.

Wavelength (nm)	**Diameter of Airy Disk (μm)**	**Diameter encircling 85% of energy (μm)**	**Diameter encircling 90% of energy (μm)**
380	not visible	3.3	4.1
450	not visible	3.3	4.1
650	1.4	4	4.3
950	2.3	5.4	6.2